AD-755 165

MAGNETIC RARE EARTH COMPOUNDS III

Robert A. Burmeister, et al

Hewlett-Packard Company

Prepared for:

Army Missile Command
Advanced Research Projects Agency

January 1973

DISTRIBUTED BY:

NTIS

National Technical Information Service
U. S. DEPARTMENT OF COMMERCE
5285 Port Royal Road, Springfield Va. 22151

AD755165

MAGNETIC RARE EARTH COMPOUNDS III

Hewlett-Packard Company

Palo Alto, California 94304

SEMIANNUAL TECHNICAL REPORT

JANUARY 1973

Contract No. DAAH01-72-C-0996
Program Code No. 0D10

Reproduced by
NATIONAL TECHNICAL
INFORMATION SERVICE
U.S. Department of Commerce
Springfield VA 22151

DDC
RECEIVED
FEB 13 1973
B

ARPA Support Office
Research, Development, Engineering,
and Missile Systems Laboratory
U.S. Army Missile Command
Redstone Arsenal, Alabama

A Research Project Sponsored by the Advanced Research Projects Agency, Department of Defense, Washington, D.C., ARPA Order 1627

NOTICE

"This research was sponsored by the Advanced Research Projects Agency of the Department of the Defense under ARPA Order 1627 and was monitored by the US Army Missile Command under Contract Number DAAH01-72-C-0996. Views and conclusions expressed herein are the primary responsibility of the author or the contractor and should not be interpreted as representing the official opinion or policy of USAMICOM, ARPA, DOD or any other agency of the Government."

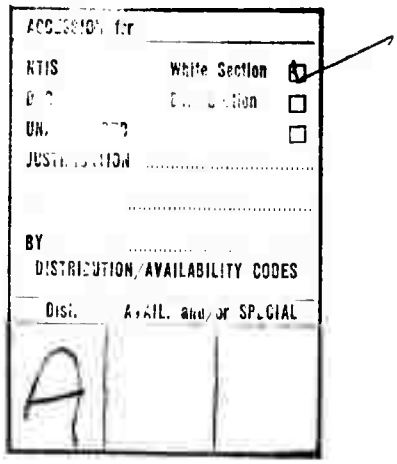

TECHNICAL REQUIREMENT NO. 1335
ARPA Order 1627

MAGNETIC RARE EARTH COMPOUNDS III

SEMIANNUAL TECHNICAL REPORT

JANUARY 1973

HEWLETT-PACKARD COMPANY
Palo Alto, California
94304
(415) 493-1501
Contract No. DAAH01-72-C-0996
Program Code No. 0D10

Monitored By
ARPA Support Office
Research, Development, Engineering, and
Missile Systems Laboratory
U.S. Army Missile Command
Redstone Arsenal, Alabama

Approved for Public Release
Distribution Unlimited

A Research Project Sponsored by the Advanced
Research Projects Agency, Department of
Defense, Washington, D. C., ARPA Order 1627

FOREWORD

This report describes work performed under Contract DAAH01-72-C-0996 for the ARPA Support Office, Research, Development, and Missile Systems Laboratory, U.S. Army Missile Command, Redstone Arsenal, Alabama during the period June 14, 1972 through December 14, 1972. The monitors for this project were S. L. Johnston and J. Shelton. The work was performed in the Solid-State Laboratory of Hewlett-Packard Laboratories under the direction of P. E. Greene. The work was supervised by R. A. Burmeister and this report was written by R. Hiskes.

The author gratefully achnowledges the assistance of R. B. Clover, L. Cutler, R. L. Lacey and R. Waites with the magnetic characterization of films. T. L. Felmlee polished the substrates and performed the optical absorption and lattice parameter measurements. F. Perlaki and L. Small helped design, construct and operate the crystal growth apparatus.

SUMMARY

The magnetically uniaxial rare earth iron garnet $(Gd,Y,Yb)_3$ $(Ga,Fe)_5O_{12}$ has been grown on {111} $Gd_3Ga_5O_{12}$ substrates. The liquid phase epitaxial dipping technique with horizontal substrate rotation has been employed in conjunction with $PbO-B_2O_3$ and $BaO-B_2O_3-BaF_2$ solvents in the temperature range of 900°C-1050°C.

Growth parameters in the BaO-based solvent, including growth temperature, undercooling and rotation rate, have been correlated with changes in growth rate and properties of the films. The distribution coefficient of gallium has been found to be relatively insensitive to growth rate and only moderately sensitive to growth temperature in this solvent, in contrast to the PbO-based solvent.

The films have been characterized with respect to composition, impurity content, lattice parameter, optical properties and magnetic properties. Films of similar composition grown in each solvent have comparable magnetic properties, but the optical absorption coefficient, lattice parameter and impurity content are higher in the epitaxial layers grown in the $PbO-B_2O_3$ solvent.

DOCUMENT CONTROL DATA - R&D
(Security classification of title, body of abstract and indexing annotation must be entered when the overall report is classified)

1 ORIGINATING ACTIVITY (Corporate author)
Hewlett-Packard Company
1501 Page Mill Road
Palo Alto, California 94304

2a REPORT SECURITY CLASSIFICATION
Unclassified

2b GROUP

3 REPORT TITLE
MAGNETIC RARE EARTH COMPOUNDS III

4 DESCRIPTIVE NOTES (Type of report and inclusive dates)
Semiannual Technical Report (June 14, 1972 to December 14, 1972)

5 AUTHOR(S) (Last name, first name, initial)
Burmeister, Robert A.
Hiskes, Ronald

6 REPORT DATE
January 1973

7a TOTAL NO. OF PAGES
50

7b NO. OF REFS
20

8a CONTRACT OR GRANT NO.
DAAH01-72-C-0996

b PROJECT NO.
Technical Requirement No. 1335

c Program Code No. 0D10

d ARPA Order No. 1627

9a ORIGINATOR'S REPORT NUMBER(S)

9b OTHER REPORT NO(S) (Any other numbers that may be assigned this report)

10 DISTRIBUTION STATEMENT
Approved for public release; distribution unlimited.

11 SUPPLEMENTARY NOTES

12 SPONSORING MILITARY ACTIVITY
Advanced Research Projects Agency
Department of Defense,
Washington, D.C., ARPA Order 1627

13 ABSTRACT

The magnetically uniaxial rare earth iron garnet $(Gd,Y,Yb)_3(Ga,Fe)_5O_{12}$ has been grown on {111} $Gd_3Ga_5O_{12}$ substrates. The liquid phase expitaxial dipping technique with horizontal substrate rotation has been employed in conjunction with $PbO-B_2O_3$ and $BaO-B_2O_3-BaF_2$ solvents in the temperature range of 900°C-1050°C.

Growth parameters in the BaO-based solvent, such as growth temperature, undercooling, and rotation rate have been correlated with changes in growth rate and properties of the films. The distribution coefficient of gallium has been found to be relatively insensitive to growth rate and only moderately sensitive to growth temperature in this solvent, in contrast to the PbO-based solvent.

The films have been characterized with respect to composition, impurity content, lattice parameter, optical properties and magnetic properties. Films of similar composition grown in each solvent have comparable magnetic properties, but the optical absorption coefficient, lattice parameter and impurity content are higher in the epitaxial layers grown in the $PbO-B_2O_3$ solvent.

DD FORM 1 NOV 68 1473 REPLACES DD FORM 1473, 1 JAN 64, WHICH IS OBSOLETE FOR ARMY USE.

14. KEY WORDS	LINK A		LINK B		LINK C	
	ROLE	WT	ROLE	WT	ROLE	WT
Garnets						
P- e Earths						
Magnetic Bubbles						
Liquid Phase Epitaxy						
BaO-based Solvents						
Crystal Growth						

TABLE OF CONTENTS

Section	Title	Page
1.0	INTRODUCTION	1
2.0	CRYSTAL GROWTH	5
2.1	Introduction	5
2.1.1	General Requirements for Reproducibility in Liquid Phase Epitaxial Crystal Growth	5
2.1.2	Garnet Composition and Substrate Selection	10
2.1.3	Crystal Growth Solvents	10
2.2	Experimental Procedures	12
2.2.1	Crystal Growth	12
2.2.2	Results and Discussion of Growth in BaO-based Solvents	14
2.2.3	Results and Discussion of Growth in the $PbO-B_2O_3$ Solvent	22
3.0	CHARACTERIZATION AND EVALUATION	23
3.1	Film Surface Morphology and Magnetic Defect Density	23
3.2	Film Composition	26
3.3	Lattice Parameter	29
3.4	Optical Measurements	31
3.5	Film Thickness and Magnetic Characterization	33
4.0	CONCLUSIONS	41
	REFERENCES	43
	DISTRIBUTION LIST	45

LIST OF ILLUSTRATIONS

Figure	*Title*	*Page*
Figure 1a.	Fluid motion induced by a horizontally rotating disk in a stationary crucible.	7
Figure 1b.	Natural fluid convection caused by the radial thermal gradients indicated by the isotherms.	7
Figure 2.	Liquid Phase Epitaxial Growth Apparatus.	13
Figure 3.	Effect of rotation rate upon the growth rate of garnet films grown in BaO-based solvent at 1020°C.	18
Figure 4.	Effect of undercooling upon the growth rate of garnet films grown in BaO-based solvent at constant rotation rate (120 rpm).	18
Figure 5a.	Fringe pattern in $(Gd,Y,Yb)_3$ $(Ga,Fe)_5O_{12}$ grown in BaO-based solvent. Film thickness 3.2 μm. Na illumination (λ = 5890 Å).	19
Figure 5b.	Fringe pattern in $(Gd,Y,Yb)_3$ $(Ga,Fe)_5O_{12}$ grown in PbO-based solvent. Film thickness 3.2 μm. Na illumination (λ = 5890 Å).	19
Figure 6.	Variation of Characteristic Length with Growth Rate for $(Gd,Y,Yb)_3$ $(Ga,Fe)_5O_{12}$ grown at 1020°C. (Open circles represent films from first batch of solution, darkened circles the second batch of solution).	20
Figure 7a.	Pits surrounded by mesas in epitaxial layer of $(Gd,Y,Yb)_3$ $(Ga,Fe)_5O_{12}$ grown in $PbO-B_2O_3$ solvent. (Bright field illumination, 500X).	25
Figure 7b.	SEM photograph of a pit in the epitaxial layer shown in Figure 6a. (4500X)	25
Figure 8	Optical Absorption Curves for Garnet Films.	32
Figure 9.	Magnetic bubble velocity in $(Gd,Y,Yb)_3$ $(Ga,Fe)_5O_{12}$ grown in $BaO-B_2O_3-BaF_2$ solvent as a function of drive field determined by the bubble translation technique.	38

LIST OF TABLES

Table	*Title*	*Page*
Table I.	Typical Specifications for Magnetic Bubble Materials	2
Table II.	Properties of PbO-based and BaO-based Solvents	11
Table III.	Representative Solution Compositions for LPE Growth of $(Gd,Y,Yb)_3$ $(Ga,Fe)_5O_{12}$	13
Table IV.	Growth Parameters for LPE Garnet Growth in $BaO-B_2O_3-BaF_2$ Solvent	15
Table V.	Reproducibility Data for $(Gd,Y,Yb)_3$ $(Ga,Fe)_5O_{12}$ grown in $BaO-B_2O_3-BaF_2$ Solvent at 1020°C.	20
Table VI.	Garnet Film Compositions	28
Table VII.	Characterization Techniques for Magnetic Rare Earth Iron Garnets	34
Table VIII.	Properties of Epitaxial Layers grown in $BaO-B_2O_3-BaF_2$ and $PbO-B_2O_3$ Solvents	36
Table IX.	Comparison of Properties of Bubble Garnets grown in BaO-based and PbO-based Solvents	40

SECTION I

1.0. INTRODUCTION

The rapid expansion of magnetic bubble technology has led to the development of the rare earth iron garnets,[1] thin films of which exhibit the magnetic uniaxial anisotropy necessary to sustain small mobile cylindrical domains or "bubbles." The films must be of uniform composition and thickness over the active device area and must be free of most common crystallographic imperfections to ensure predictable response of the bubbles to applied magnetic forces. Epitaxial liquid phase growth techniques have proved successful in meeting most of the material specifications shown in Table I.

In view of the potential technological importance of these devices and the key role of magnetic rare earth compounds, this program was undertaken in an effort to advance the state-of-the-art in the science and technology of these materials. The specific objectives of this program include the following:

1. Development of practical techniques for the growth of single crystals of rare earth compounds having properties suitable for studies and utilization of bubble domain phenomena.
2. Acquisition of the necessary data to better characterize and quantitatively describe both the crystal growth process and the salient physical and chemical properties of the crystals produced.
3. Determination of the relationship between methods and parameters of the crystal growth process and relevant physical properties of the crystals thus grown.

Table I. Typical Specifications for Magnetic Bubble Materials

MATERIAL PROPERTY	SPECIFICATION	RELATED DEVICE OPERATING CHARACTERISTICS
Film Thickness Run to run variation Variation over the film	3.0 - 4.0 μm ±5% ±1%	Bit Size Bit Density
Bubble Diameter	6 μm	
Bubble Ellipticity	< 0.2	
Characteristic Length Run to run variation Variation over the film	0.8 μm ± 5% ± 1%	A compromise between drive field power requirements, ease of detection, and bubble size and stability
Saturation Magnetization Run to run variation Variation over the film	75-150 Gauss ± 5% ± 1%	
Anisotropy Field	>2 •Magnetization	
Mobility	>200 cm/Oe-sec	Data Rate
Coercive Force	<0.3 Oe	
Temperature Coefficient of Characteristic Length	<0.001 μm/°K	Operating stability over 50°K temperature range
Density of Crystal Defects Which Affect Magnetic Properties	< $5/cm^2$	Reliable predictable bubble propagation, high yield of large chips
Usable Defect Free Area	> 25 mm^2	

To meet these objectives we have developed a new solvent, comprised of BaO, B_2O_3 and BaF_2 for the solution growth of these compounds.[2,3] Growth parameters have been explored for state-of-the-art crystal growth techniques in this solvent, including (1) steady state temperature gradient homoepitaxial growth of $YFeO_3$ and (2) heteroepitaxial growth of the rare earth iron garnets $(Eu,Er)_3\ (Ga,Fe)_5O_{12}$ and $(Gd,Y,Yb)_3\ (Ga,Fe)_5O_{12}$ by the dipping technique with horizontal substrate rotation. In the present contract period the growth temperature, undercooling and substrate rotation rate have been correlated with growth rate, thickness uniformity, and magnetic properties of the heteroepitaxial garnet films.

The limitations of conventional PbO-based solvents have been explored, and films of nearly the same composition grown in the PbO-based and BaO-based solvents have been compared with respect to impurity content, lattice parameter, optical density and magnetic properties. In some cases significant differences have been found in these properties.

The choice of materials to be grown has been dictated by the current state-of-the-art knowledge of the magnetic bubble materials, and in the present contract period materials studies have focused on the rare earth iron garnet $(Gd,Y,Yb)_3\ (Ga,Fe)_5O_{12}$, which exhibits the necessary uniaxial anisotropy with a proper stable bubble size of 4-8μm.

The characterization studies necessitated the development of techniques to fully explore the properties of the rare earth iron garnets. These techniques included (1) defect studies by an AC optical method, Lang and Berg-Barrett topography, as well as an etching technique, (2) impurity content and film compositon by microprobe and emission

spectrographic analysis, (3) lattice mismatch by X-ray diffractometry, (4) film thickness and thickness uniformity by interferometry, (5) optical absorption, and (6) a full range of magnetic measurements including magnetization, characteristic length, wall energy, anisotropy energy, mobility, coercive force, Néel temperature, and the temperature dependence of the magnetic properties.

SECTION II

2.0. CRYSTAL GROWTH

2.1. Introduction

Although rare earth garnets have been grown by a variety of techniques, the most promising method for materials to be used for magnetic bubble device applications has been that of epitaxial growth on a paramagnetic transparent substrate, including both liquid phase epitaxial (LPE) and vapor phase epitaxial (VPE) growth (also referred to as chemical vapor deposition (CVD)). We have chosen LPE because it is an inherently simple and reliable process when used with a stable solvent, and one which permits precise interface temperature and temperature gradient control when properly implemented. The LPE process also permits the use of growth induced magnetic anisotropy in materials design. This flexibility is not possible in VPE, which requires stress induced by a film/substrate lattice parameter mismatch to produce the necessary uniaxial anisotropy.

2.1.1. General Requirements for Reproducibility in Liquid Phase Epitaxial Crystal Growth

The growth process is one of the most critical factors influencing the magnetic properties of the epitaxial layer. Proper control of the process involves a quantitative understanding of the relationships between crystal morphology, composition and perfection, and the solid-liquid interface variables[4]. These variables are related to the controllable macroscopic system variables, such as growth temperature, fluid motion, fluid composition, and growth time, by the solutions to the relevant boundary value problems.

Although these boundary value problems are in general quite complicated since they involve a moving boundary with coupled phase transformation, heat flow and mass flow, approximate solutions have been developed for one practical type of growth process, that of growth on a rotating horizontally held substrate immersed in a supersaturated isothermal nutrient solution.[6,7] The model assumes an infinite disk rotating in a semi-infinite solution and a diffusion limited growth rate which is determined by the motion of the slowest crystal constituent through a stagnant boundary layer adjacent to the crystal interface.

A rotating substrate in a cylindrical crucible produces the fluid motion shown in Figure 1a,[8] where the boundary layer δ can be maintained constant over the entire surface of the substrate (except for edge effects) by rotating at a rate high enough to overcome the natural convection flow pattern shown in Figure 1b caused by the radial temperature gradient in the crucible (the wall is hotter than the center). The width and uniformity of this boundary layer are critical in determining the epitaxial layer growth rate and thickness uniformity. The solute boundary layer width for this model is given by[9]

$$\delta = 1.6\, D^{1/3}\, \nu^{1/6}\, r^{-1/2} \qquad (1)$$

where D is the diffusion coefficient, ν is kinematic viscosity and r is rotation rate. The growth rate can be related to the boundary layer through an analysis developed by Ghez and Giess[7]

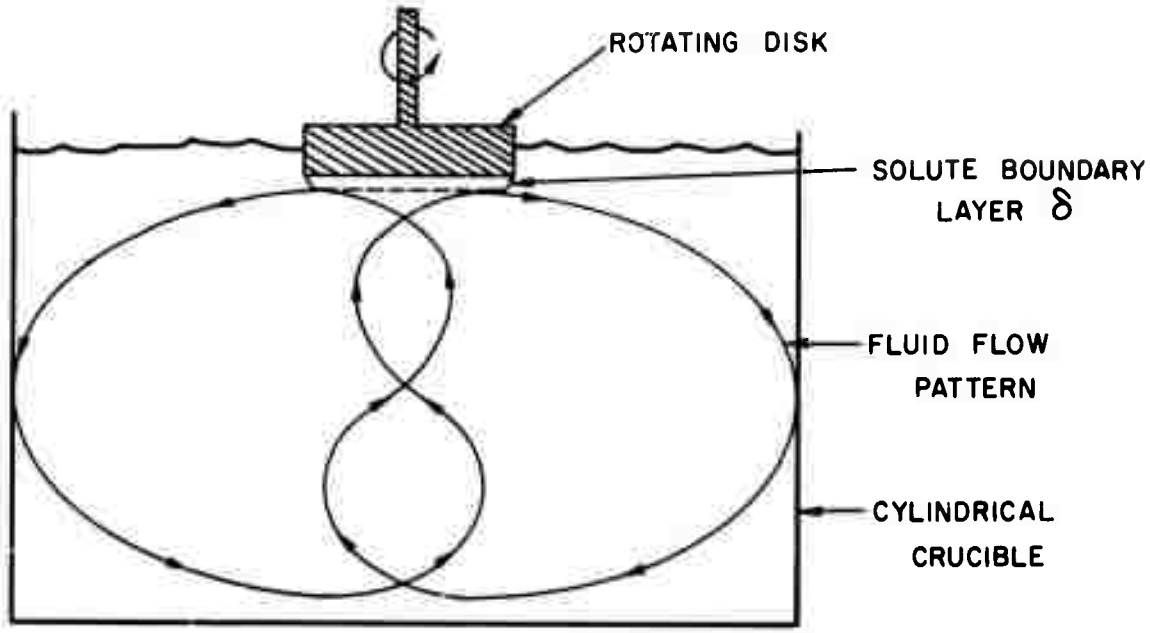

Figure 1a. Fluid motion induced by a horizontally rotating disk in a stationary crucible.

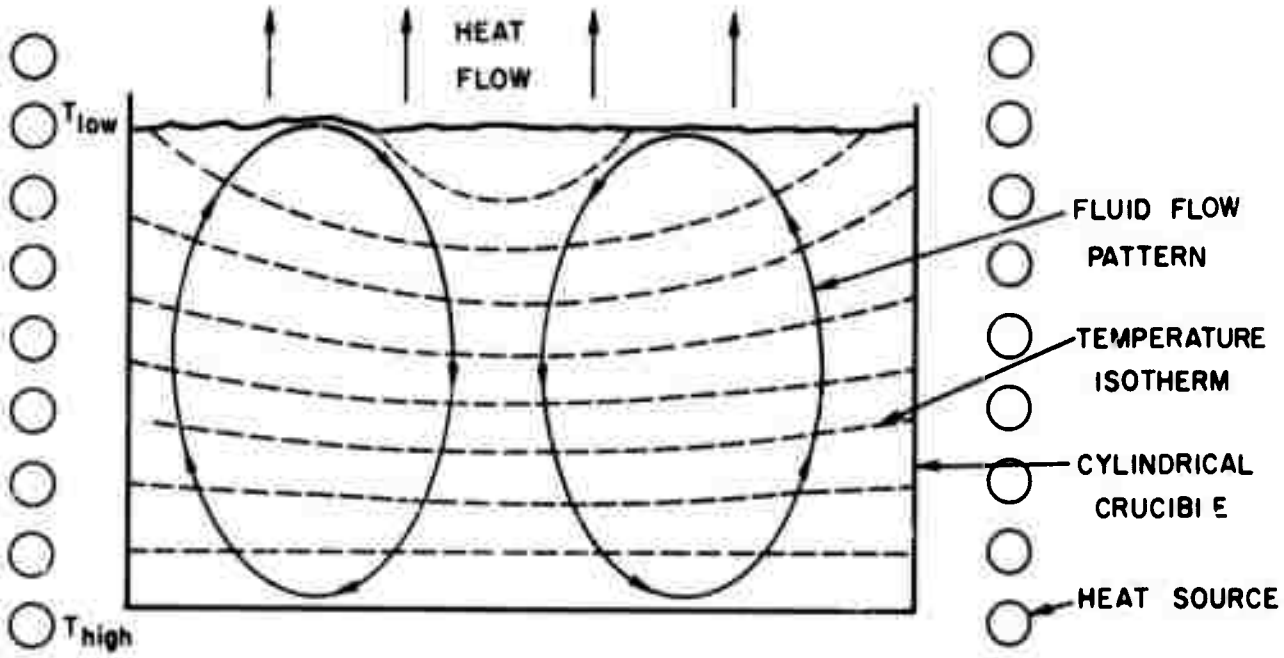

Figure 1b. Natural fluid convection caused by the radial thermal gradients indicated by the isotherms.

$$V = \frac{D(C_L - C_E)}{\rho\delta}\left[\frac{1}{1+R} + 2\sum_{n=1}^{\infty}\frac{\exp(-\alpha_n^2 Dt/\delta^2)}{(1+R+R^2\alpha_n^2)}\right] \qquad (2)$$

where C_L = the solute concentration of the slowest diffusing constituent in the multicomponent bulk liquid,

C_E = the equilibrium solute concentration of this constituent,

ρ = density of the epitaxial film,

D = diffusion coefficient of the slowest diffusing crystal constituent,

K = the first order rate constant of the interface reaction,

R = $D/\delta K$, a parameter measuring the relative importance of diffusion to reaction,

α = the positive nonzero roots of the equation $\tan\alpha + R\alpha = 0$, and

t = time.

Equation (2) predicts an initial transient stage of epitaxial growth (during which the second term dominates) which decays exponentially to a steady-state growth rate given by the first term for rotation rates > 0. The theory predicts a growth rate which varies parabolically with the rotation rate and linearly with supersaturation. If the liquidus curve is assumed to be a straight line, the growth rate at fixed rotation rate should also vary linearly with undercooling. Such a correlation has been attempted in the PbO-based solvent by Giess et al.[6] In general, however, the liquidus curve is best described by $C_E = C_0 e^{-\Delta H/RT}$ where ΔH and R are constants,[10,11] and it is readily shown that the growth rate should be proportional to $(T_S - T_G)/T_G$, where T_S is the saturation temperature and T_G is the growth temperature. These assertions have been shown to be valid for the BaO-based solvent as will be discussed in Section 2.2.2.

This analysis also points out the variables that must be controlled for adequate reproducibility of growth rate and film thickness. The most important of these are the supersaturation (C_L-C_E), the boundary layer width δ and the growth time t. The rotation rate (which has the greatest effect on δ) and t can easily be controlled to ±1 rpm and ±5 sec respectively, which are consistent with the reproducibility requirements in Table I. The parameter most difficult to control is the supersaturation, which is determined both by the growth temperature (which can be controlled to ±0.3°C) and by the presence or absence of crystallites growing elsewhere in the crucible. Spurious nucleation leads to irreproducible thickness and magnetic properties of the epitaxial film. It is best avoided by (1) using crucible and holder geometry which do not contain sites of easy nucleation, (2) operating at low values of undercooling, and (3) vigorously stirring the solution above the saturation temperature before growth to ensure complete dissolution of all constituents.

These conditions have been met with adequate care on the part of the crystal grower, and the resultant run-to-run variations in thickness, characteristic length and magnetization are currently within the requirements shown in Table I for films grown in either the PbO-B_2O_3 or BaO-B_2O_3-BaF_2 solvent. Reproducible growth in the BaO-B_2O_3-BaF_2 solvent will be demonstrated in Section 2.2.2.

2.1.2. Garnet Composition and Substrate Selection

Garnet compositions must be carefully selected to meet the stringent materials requirements listed in Table I, and perhaps the most critical control is needed in matching substrate and film lattice parameters. $Gd_3Ga_5O_{12}$ has been chosen as the substrate material for this program since it is commercially available in the quality and quantity needed for liquid phase epitaxial growth, although there is no fundamental reason why bubble garnets could not be grown on another substrate such as $Y_3Al_5O_{12}$.

In the current contract period, attention has focused on the garnet composition $(Gd,Y,Yb)_3\ (Fe,Ga)_5O_{12}$ for two reasons; (i) it has the potential to satisfy the requirements listed in Table I and therefore is of great practical interest, and (ii) it is representative of the entire class of rare earth iron garnets, and therefore the development of techniques for its proper growth and characterization may be applicable to the entire class of garnets.

2.1.3. Crystal Growth Solvents

There are two solvent systems currently used for the growth of the rare earth iron garnets, the PbO-based and BaO-based solvents. Each solvent has certain advantages and disadvantages as shown in Table II. The principle advantage of the $PbO\text{-}B_2O_3$ solvent is its low viscosity at growth temperaturesas low as 800°C, which permits complete runoff of solution after crystal growth. The higher viscosity of the $BaO\text{-}B_2O_3\text{-}BaF_2$ solution, on the other hand, makes solution removal more difficult, but is advantageous

Table II. Properties of PbO-Based and BaO-Based Solvents.

	$BaO-B_2O_3-BaF_2$	$PbO-B_2O_3$
Volatility	Negligible at 1450°C	Considerable at 900°C
Viscosity	Relatively high at temperatures less than 1000°C	Low down to 800°C
Chemical Reactivity with Platinum	Negligible	Reacts readily if free lead is present
Density	Less than magnetic bubble materials (~ 4.7 gm/cm^3)	Greater than magnetic bubble materials (~ 6 gm/cm^3)
Solubility of Magnetic Garnets	~ 18 mole % at 1000°C, 2-3 times greater than $PbO-B_2O_3$ solvent	~ 7.3 mole % at 940°C
Garnet Phase Saturation	Congruent	Incongruent
Solvent Incorporation (Decreases with increasing temperature)	0.01 wt. % Ba at 990°C growth temperature	0.2 wt. % Pb at 900°C growth temperature
Gallium Distribution Coefficient	$\alpha_{Ga} \approx 1$	$\alpha_{Ga} = 1.6\text{-}2.5$

during growth because it does not respond as readily to thermal instabilities in the fluid, such as the tendency for natural convection shown in Figure 1b. The higher viscosity has a minor effect on the boundary layer thickness during growth since it enters as the 1/6 power in Equation 1. The primary advantages of the BaO-based solvent are its low volatility and chemical reactivity with the platinum crucible, and the high garnet solubility. The low volatility aids run-to-run reproducibility and the low chemical reactivity inhibits platinum incorporation into the film, which can affect the lattice parameter and defect density, and hence the magnetic properties of the film.

2.2. Experimental Procedures

2.2.1. Crystal Growth

The growth techniques were very similar in both the $PbO\text{-}B_2O_3$ and $BaO\text{-}B_2O_3\text{-}BaF_2$ solvents. The 0.75" diameter Syton* polished $Gd_3Ga_5O_{12}$ substrates were dipped into ~250 gm of growth solution contained in 100 cc platinum crucibles as shown in Figure 2. Representative solution compositions are shown in Table III. In the $PbO\text{-}B_2O_3$ solvent, two values of the ratio $R_1 = \frac{Fe_2O_3}{\Sigma Ln_2O_3}$† were used, $R_1 = 9$ and $R_1 = 14$. This ratio was maintained at $R_1 = 1.1$ in the BaO-based solution. The solute concentration in the $PbO\text{-}B_2O_3$ solution was varied from 7.306 mole% for $R_1 = 9$ to 8.683 mole% for $R_1 = 14$, and as a result the saturation temperature varied from 940°C ±7°C to 925°C ±2°C (as determined by substrate dipping experiments). In the BaO-based solvent the solute concentration was maintained at 19 mole% resulting in a saturation temperature of 1060°C ±7°C.

The solutions were prepared by first melting the premixed dried solvent constituents at 1100°C and then dissolving the premixed solute at 1200°C for 24 hours. The solutions were equilibrated before each growth run for a minimum of

*A Product of The Monsanto Company

† Ln represents rare earths + yttrium

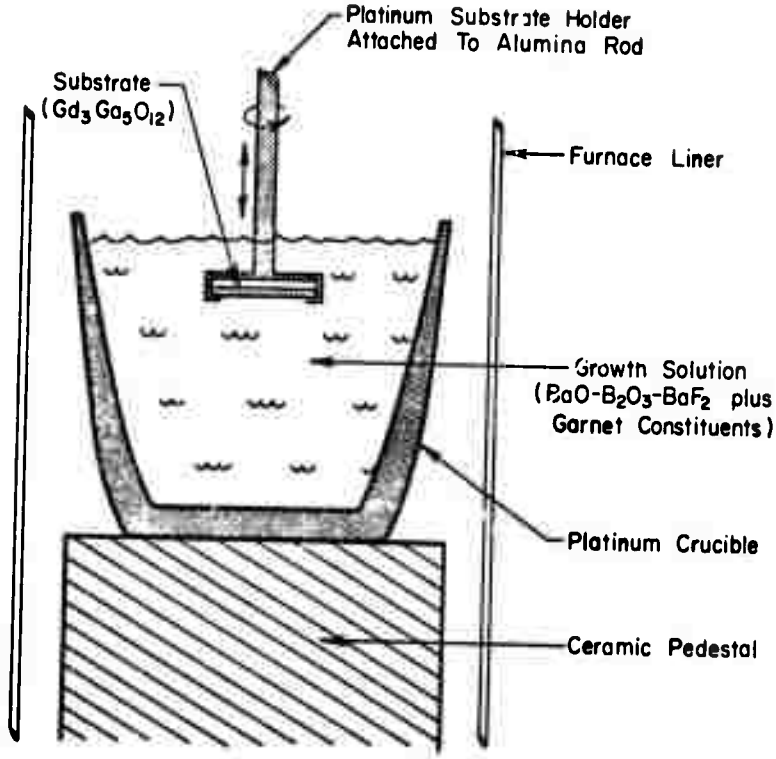

Figure 2. Liquid Phase Epitaxial Growth Apparatus.

Table III. Representative Solution Compositions for LPE Growth of $(Gd,Y,Yb)_3(Ga,Fe)_5O_{12}$

$PbO-B_2O_3$ Solvent (grams)		$BaO-B_2O_3-BaF_2$ Solvent (grams)
PbO	230.7500	
B_2O_3	4.6116	41.5051
$BaCO_3$	-	117.6169
BaF_2	-	45.8789
Fe_2O_3	14.0708	25.7202
Ga_2O_3	1.9107	6.7766
Gd_2O_3	0.5323	12.2286
Y_2O_3	0.7343	16.8696
Yb_2O_3	0.6200	14.2436
$Fe_2O_3/\Sigma Ln_2O_3$	14 (mole ratio)	1.1 (mole ratio)
Solute Concentration	8.683 Mole %	19.000 mole %

1 hour at 1100°C with constant stirring. The BaO-based solution was also maintained between runs at 1100°C with constant stirring. The PbO-based solution was maintained at 985°C between runs to minimize solvent loss by vaporization.

Initial growth runs were performed by dipping the substrates vertically into a quiescent solution followed by a slow (1cm/min) withdrawal from the solution to ensure solution removal after growth. Most of the growth runs, however, were performed with substrates held horizontally and rotated during growth at speeds up to 200 rpm. After growth, the substrates were rotated at 200 rpm for PbO-based solution removal and at 2000 rpm for BaO-based solution removal. 2000 rpm was sufficient to remove all but a small ring of the BaO-based solution at the periphery of the layer. The films were subsequently withdrawn from the furnace at a rate of 5 cm per minute, and the remaining solution was etched off with 30% acetic acid at 80°C.

The growth temperature in the $PbO-B_2O_3$ solution was maintained at 900°C ±0.3 °C for all growth runs, but was varied from 990°C-1050°C in the BaO-based solution. All the growth runs were isothermal except for a few cooling runs in the BaO-based solution from 1040-990°C.

2.2.2. Results and Discussion of Growth in BaO-based Solvents

The growth parameters for representative LPE growth runs of $(Gd,Y,Yb)_3(Ga,Fe)_5O_{12}$ illustrating the variation in growth rate with growth temperature and rotation rate are shown in Table IV. The saturation temperature for all the films was 1060°C ±7°C, and all except the one grown by slow cooling were grown from the same batch of solution and were

Table IV. Growth Parameters for LPE Garnet Growth in $BaO-B_2O_3-BaF_2$ Solvent.

Solution Composition	Run Temp. (°C)	Growth Rate (μm/min)	Rotation (rpm)	Thickness (μm)
$Gd_{.7}Y_{1.55}Yb_{.75}Ga_{.9}Fe_{4.1}O_{12}$	1020	.76	200	5.8
"	1020	.70	120	3.5
"	1020	.43	50	3.3
"	1020	.21	0	1.6
"	990	1.02	120	5.1
"	1040	.29	120	2.9
"	1050	.13	120	3.0
"	1040→990	.16	0	3.6

held horizontally. The solutions were equilibrated for periods varying from 2 to 18 hours at 1100°C with constant stirring prior to growth. Initial experiments in which the solutions were equilibrated for 2 hours at 1100°C without stirring produced thin films of irreproducible thickness, which indicated incomplete dissolution with attendant crystal growth elsewhere in the crucible during the growth run. Stirring during the 2 hour equilibration, however, produced films with predictable and reproducible thickness which indicated the absence of spurious crystallization in the solution. There was no difference in growth rate between a 2 hour and an 18 hour equilibration, implying that 2 hours is sufficient.

Although spontaneous nucleation can be readily detected in the PbO-based solution by observation of crystallites floating on the surface, this is not possible in the BaO-based solution because it is less dense than either garnet or orthoferrite. Spurious crystal growth can be detected in either solution by examination of the crucible walls for crystallites after the solution is poured out at the conclusion of a series of growth runs. No such crystals were ever found growing on the crucible wall. Occasionally, small garnet and orthoferrite crystallites were found on the surface of the epitaxial film, but these could be easily moved about or wiped off, and were presumed to have originated from spontaneous nucleation in the ring of solution remaining on the periphery of the film and on the substrate holder itself as the assembly cooled during removal from the furnace. These small crystallites were then presumably leached out during etching and stuck to the epitaxial layer. The presence of orthoferrite as well as garnet crystals is not surprising since an R_1 of 1.1 must be close to the orthoferrite phase boundary and it is possible for the solution to approach the phase boundary upon cooling.

The effects of rotation rate upon film thickness and growth rate are shown in Table IV and Figure 3. The growth rate varies linearly with the square root of rotation rate with a positive intercept at the origin as predicted by Equation 2. Figure 4 shows that at constant rotation rate the growth rate also varies linearly with $\Delta T/T$ and passes through the origin, which is predicted by the analysis if the liquidus curve is exponential.[11] The thickness uniformity of horizontally rotated films did not depend strongly upon rotation rate in either solvent, and the variation was generally less than 5% of the thickness of the film over >50% of the area as shown in Figure 5.

Reproducibility in the $BaO-B_2O_3-BaF_2$ solvent is demonstrated in Table V which shows the results of a series of 20 growth runs over a period of 19 days in one batch of solution plus another 3 growth runs in a fresh batch of solution. The growth temperature was held constant (1020°C) during this period and the film thickness and growth rate were varied by changing the rotation rate and growth time. All the films were grown from the same batch of solution, which was equilibrated at 1100°C between runs. The growth rate varied from 0.21 μm/min to 1.12 μm/min and the thickness varied from 1.6 μm to 8.5 μm. Despite this wide variation in growth rate, the magnetic properties remained remarkably constant. The Néel temperature of 163°C ±1°C is within the error of the measurement as is the magnetization of 163 gauss ±10% (except for run number 10). There is, however a slight upward trend in magnetization with increasing growth rate. This trend can be more easily detected in the variation of the characteristic length (ℓ) with

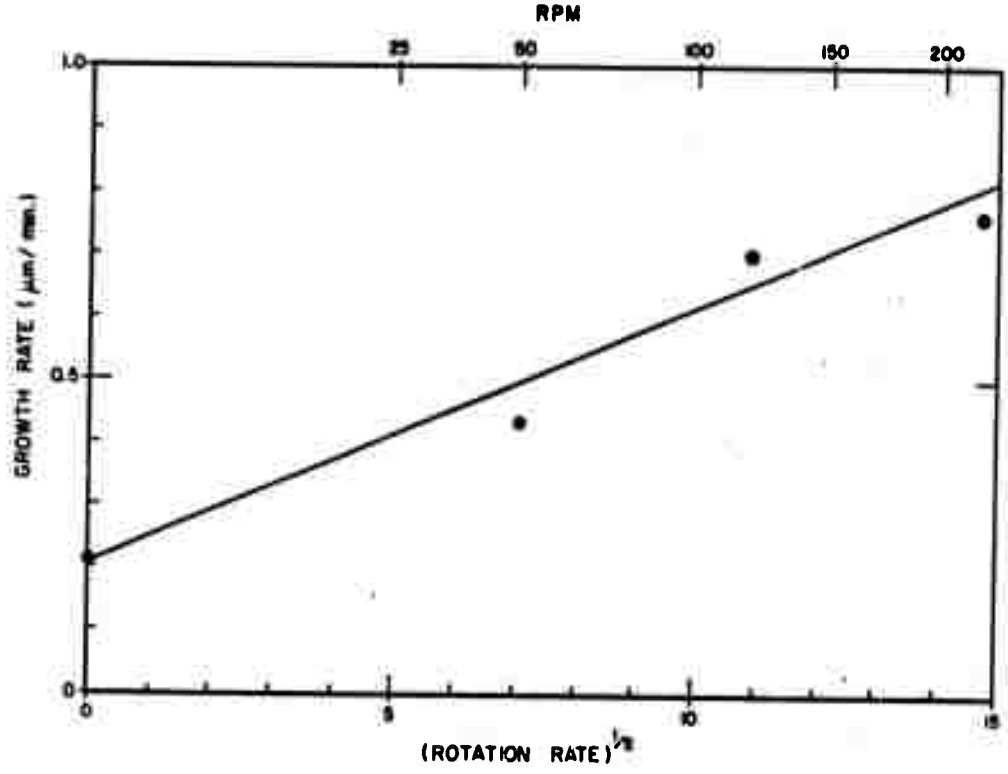

Figure 3. Effect of rotation rate upon the growth rate of garnet films grown in BaO-based solvent at 1020°C.

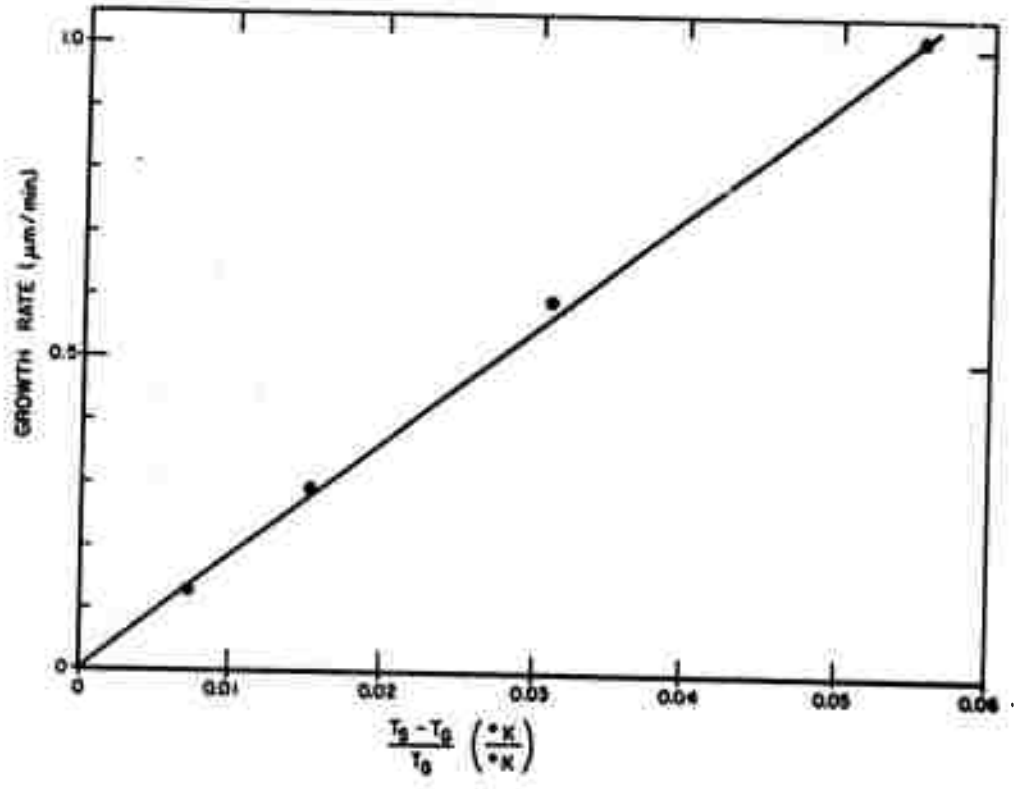

Figure 4. Effect of undercooling upon the growth rate of garnet films grown in BaO-based solvent at constant rotation rate (120 rpm).

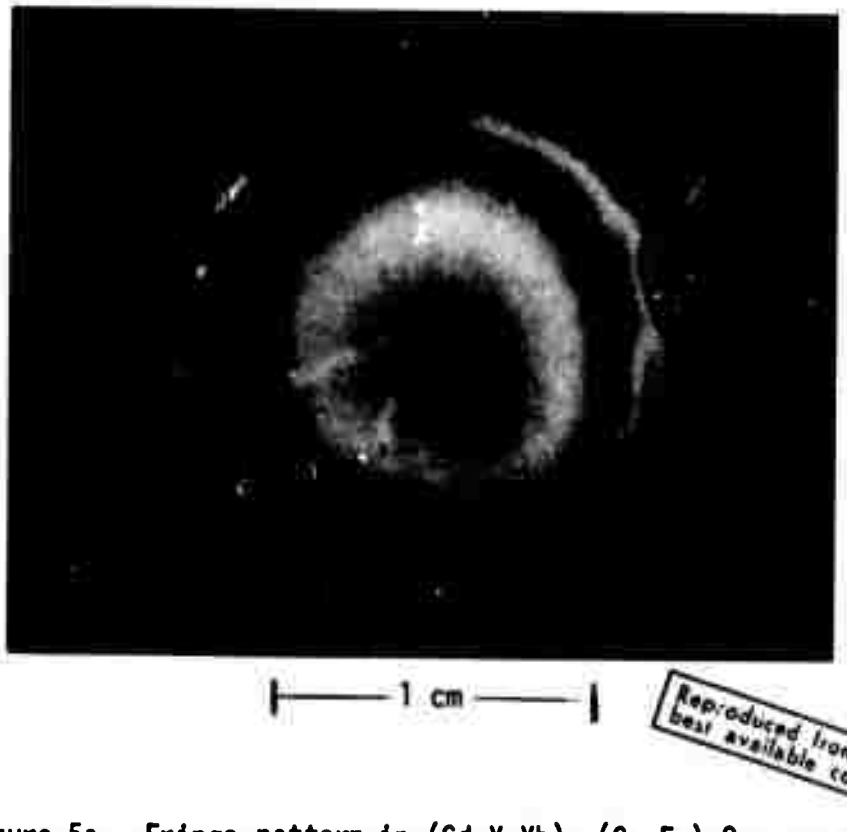

Reproduced from best available copy.

Figure 5a. Fringe pattern in $(Gd,Y,Yb)_3$ $(Ga,Fe)_5O_{12}$ grown in BaO-based solvent. Film thickness 3.2 μm. Na illumination (λ = 5890Å).

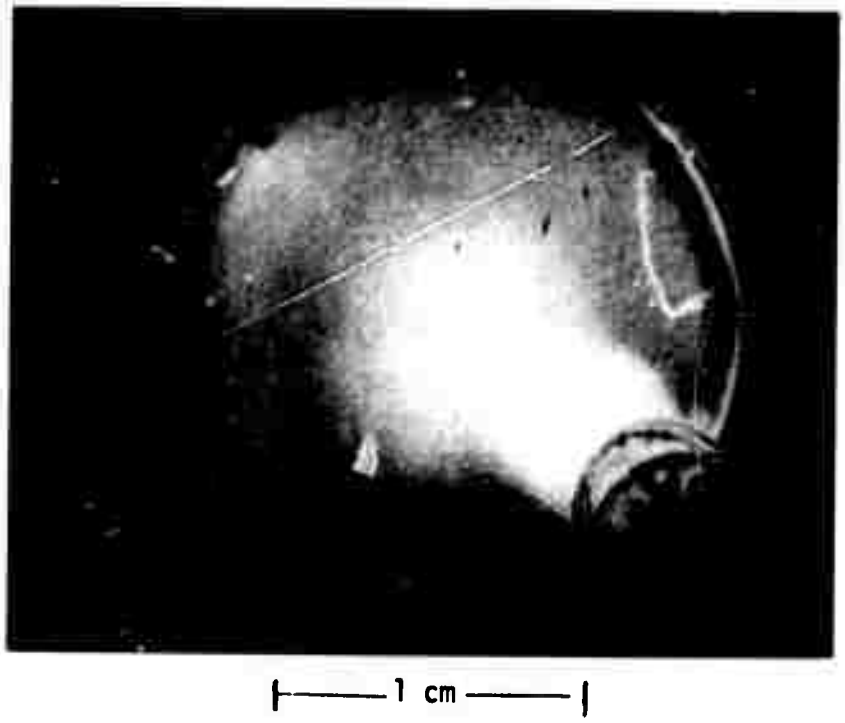

Figure 5b. Fringe pattern in $(Gd,Y,Yb)_3$ $(Ga,Fe)_5O_{12}$ grown in PbO-based solvent. Film thickness 3.2μm. Na illumination (λ = 5890Å).

Table V. Reproducibility Data for $(Gd,Y,Yb)_3(Ga,Fe)_5O_{12}$ Grown in $BaO-B_2O_3-BaF_2$ Solvent at 1020°C.

Run No.	Days Since Beginning of this Series of Runs	Growth Rate (μm/min)	h (μm)	ℓ (μm)	4πM (gauss)	σ_w ($ergs/cm^2$)	T_N (°C)
1	5	.35	6.2	.59	145	.10	162
2	5	.37	6.5	.55	146	.09	-
3	9	.54	6.8	.49	144	.08	-
4	9	.42	5.3	.58	152	.11	-
5	10	.46	3.5	.53	168	.12	164
6	10	.51	3.9	.55	167	.12	-
7	11	.51	4.2	.53	169	.13	-
8	11	.50	3.8	.54	170	.12	162
9	12	.76	5.8	.44	187	.12	-
10	16	1.12	8.5	.43	204	.14	-
11	16	.70	5.3	.51	166	.11	164
12	17	.21	6	.54	159	.11	-
13	17	.24	1.8	.57	141	.09	163
14	18	.62	4.7	.46	157	.09	163
15	19	.43	3.3	.54	147	.09	162
16	19	.41	3.1	.57	157	.11	-
17	23	.76	3.7	.48	168	.11	-
18	23	.50	2.5	.53	169	.12	-
19	24	.70	3.5	.47	161	.10	-
20	24	.68	3.4	.46	170	.11	162
	Fresh Solution						
21	3	.48	4.8	.54	160	.11	163
22	7	.70	3.5	.46	171	.11	-
23	7	.64	3.2	.49	174	.12	163
Uncertainty in the Measurement		±10%	±10%	±5%	±15%	±16%	±1°C

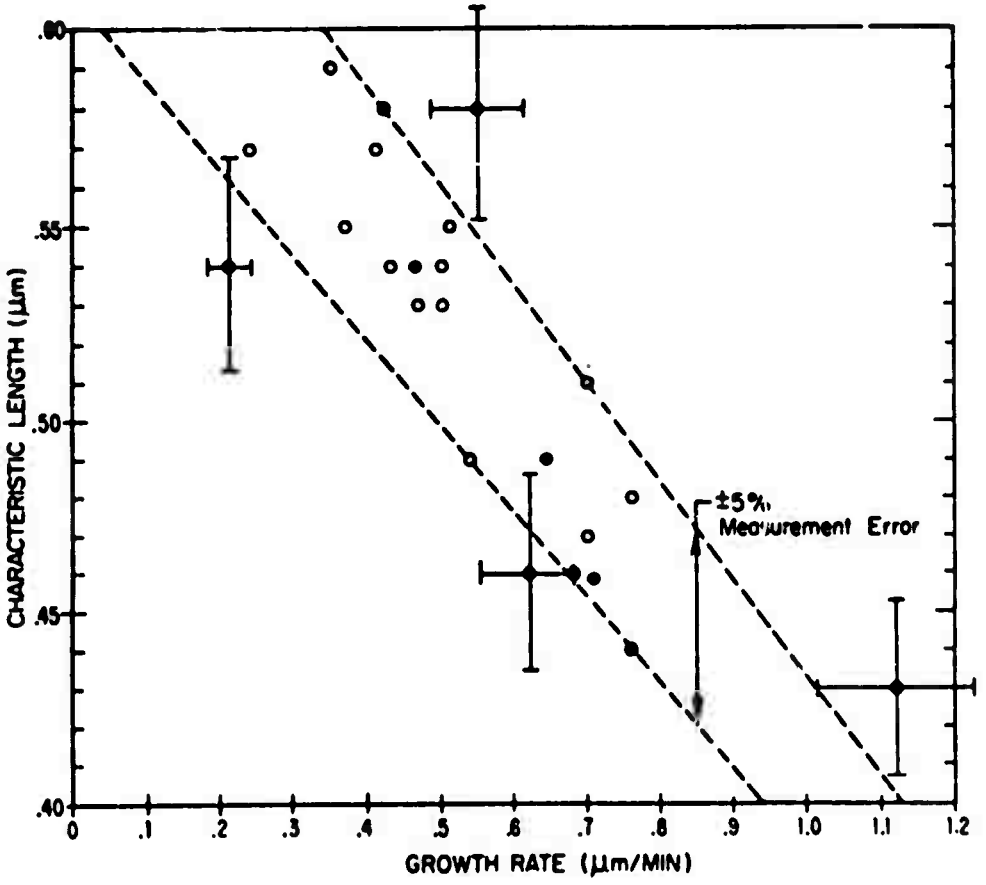

Figure 6. Variation of Characteristic Length with Growth Rate for $(Gd,Y,Yb)_3(Ga,Fe)_5O_{12}$ Grown at 1020°C. (Open circles represent films from first batch of solution, darkened circles the second batch of solution).

growth rate shown in Figure 6. The shaded region indicates only the uncertainty in the measurement of ℓ.[†] The uncertainty in both growth rate and ℓ is shown for the data lying outside the shaded region, and it can be seen that within measurement error, all the data are consistent with a decrease in ℓ of 0.025 μm for an increase in growth rate of 0.1 μm/min. Implications of this variation and comparison with films grown in the PbO-based solvent will be explored in Section 3.5. The point to be made here is the ability of the present growth process to reproduce films of predictable properties as demonstrated by the fact that all of the 23 films lie within the measurement uncertainty with respect to magnetization, Néel temperature, wall energy and characteristic length.

[†]Characterization techniques will be discussed more fully in Section III.

2.2.3. Results and Discussion of Growth in the $PbO-B_2O_3$ Solvent

A series of growth runs was carried out in the $PbO-B_2O_3$ solvent for comparison with those in the $BaO-B_2O_3-BaF_2$ solvent. Initial growth runs performed in the PbO-based solvent with the substrate held vertically did not produce epitaxial films of uniform thickness in contrast to those grown with this geometry in the BaO-based solvent.[4,5] The films were always thicker at the top even with a vertical temperature gradient of 7°C/cm (hotter at the top). This was attributed to the dominant fluid motion caused by the radial temperature gradient, and all subsequent runs were performed in the horizontal growth mode. The films were grown at 900°C (undercooling = 25°C) and a growth time of 4 minutes at 30 rpm produced films 3.7 ±0.1 μm thick. The rotation rate employed resulted in films that were flat to < ±0.15μm over 80% of the area of the 0.75" diameter substrates.

Although the value of $R_1 = 9.0$ has been reported to be in the orthoferrite phase field,[12] no evidence of orthoferrite precipitation was seen in films grown from this composition. However, as the films were withdrawn from the growth solution, small droplets of solution often remained at the junction of the substrate holder, and as these cooled, small (1-3 μm) crystallites of both orthoferrite and garnet precipitated, just as described for the case of BaO-based solutions in Section 2.2.2. This occurred for $R_1 = 9.0$ as well as $R_1 = 14.0$. The crystallites deposited on the garnet film surface as the solution was etched off in acid, and could be easily brushed off the surface. The presence of both orthoferrite and garnet crystallites suggests that the two phase boundary is reached before the solution solidifies (somewhere between the growth temperature of 900°C and the eutectic temperature of 783°C), resulting in the coprecipitation of both phases.

A comparison of some of the properties of films grown in the $PbO-B_2O_3$ solvent with those of similar composition grown in the $BaO-B_2O_3-BaF_2$ solvent will be given in Section III.

SECTION III

3.0. CHARACTERIZATION AND EVALUATION

3.1. Film Surface Morphology and Magnetic Defect Density

Flat, crack-free surfaces with low defect densities are required for successful operation of bubble devices. Cracking and macroscopic surface quality can be adequately controlled by suitable compositional choice to avoid excessive lattice mismatch as well as by proper control over the growth process. The most persistent class of defect remains the localized defect or imperfection in the garnet film. There are several sources of localized defects, (1) dislocations and inclusions in the substrate resulting from faulty growth conditions, (2) scratches or particulate matter on the surface of the substrate resulting from improper polishing and cleaning procedures, and (3) defects introduced during the epitaxial growth process. The third class of defects results from spontaneous crystallization of either garnet or orthoferrite phase with subsequent incorporation into the film. In some cases a faceted pit is formed at the site of incorporation which is difficult to distinguish from a pit originating from a substrate defect.

We have observed different defect morphologies in the BaO-based and PbO-based solvents. The only significant defects present in films grown in $BaO-B_2O_3-BaF_2$ were triangular pits, either pyramidal or flat bottomed. These pits never had surrounding mesas or raised portions of the garnet film around them, which was invariably seen in the $PbO-B_2O_3$ solvent.

The dimensions of the pits ranged from 3-10 μm and the depth varied from <0.5 μm to the depth of the film. Some of the pyramidal pits were attributed to substrate dislocations by the characteristic strain pattern when viewed between crossed polarizers, and others were caused by particulate matter on the surface. The origin of the flat bottomed pits is not clear. They may have been pyramidal pits originating at the substrate surface or in the film itself, which began to fill up as the film grew. Similar flat bottomed etch pits have been seen in improperly polished substrates which have been etched in H_3PO_4 at 160°C. The defect density in the films sometimes varied by as much as two orders of magnitude from run to run where the only variable was the substrate, and the best layers had defect free areas >20 mm^2, adequate for magnetic bubble devices. The only other prevalent defect in these films was the occasional cracking and spalling of the film around the periphery (<1 mm in from the edge) of the horizontally rotated substrates caused by solution adherence to the film. This defect can be minimized or eliminated by the 2000 rpm spin after growth.

The films grown in the $PbO-B_2O_3$ solvent exhibited a variety of defects. The pyramidal and flat bottomed pits prevalent in films grown in the BaO-based solvent were observed very infrequently. The most common defect morphology was the multifaceted pit, bounded by {211} and {110} planes, examples of which are shown in Figure 7. In addition, there were very small (< 1μm) defects barely visible as black specks in the optical microscope which however, impeded domain wall motion. All of the pits observed in these films had surrounding mesas, or circular raised portions of the garnet film as shown in Figure 7, which were caused by continuing growth from small

Reproduced from best available copy.

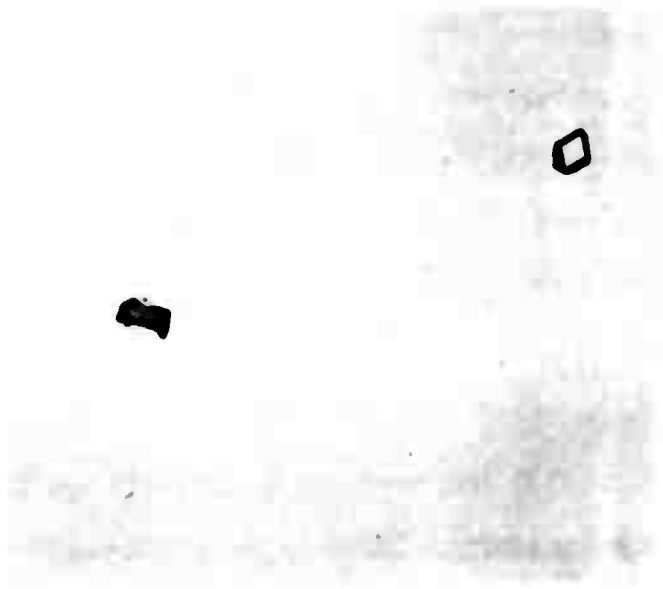

Figure 7a. Pits surrounded by mesas in epitaxial layer of $(Gd,Y,Yb)_3\ (Ga,Fe)_5\ O_{12}$ grown in $PbO\text{-}B_2O_3$ solvent. (Bright field illumination, 500X).

Figure 7b. SEM photograph of a pit in the epitaxial layer shown in Figure 6a. (4500X)

droplets which remained at the pit after withdrawal from the solution. This continuing growth process may have resulted in growth at the bottom of the pit also, producing the characteristic flat bottom. The best films were similar in quality to the best films grown in the BaO-based solvent, with defect free areas >20 mm^2.

3.2. Film Composition

Selected films were analyzed by emission spectrographic and electron microprobe analysis. These data together with measurement of Néel temperature and lattice parameter are useful in specifying not only the film composition, but also the distribution coefficients of cations between solid and liquid.

The films selected for emission spectrographic analysis were 12-15μm thick, and were prepared by lapping off the substrate to eliminate dilution effects before crushing the film. Films grown in the $PbO-B_2O_3$ solvent at 900°C at a growth rate of 0.95μm/min contained 0.18-0.20 wt. % Pb and 0.02 wt. % Pt. Films grown in the $BaO-B_2O_3-BaF_2$ solvent at 990°C at a growth rate of 0.75 μm/min contained 0.009-0.0095 wt. % Ba and <10 ppm Pt, which represents an order of magnitude reduction for both

impurities. These values of Pb and Ba incorporation are in agreement with those reported in the literature.[12,13] The smaller amount of solvent impurity in the films grown in the BaO-based solvent may be a result of the higher growth temperature, since the solubility decreases with increasing temperature, but the difference in platinum content of the films is a consequence of the more corrosive nature of the $PbO-B_2O_3$ solvent. It is not clear whether the platinum is incorporated interstitially or substitutionally, nor what effect it has on lattice parameter, defect density and magnetic properties. The Pb markedly increases the lattice parameters and alters the optical properties of the garnet films as will be shown in later sections. It is believed that the Pb enters as Pb^{2+} on the rare earth sites, causing an Fe valence change from Fe^{2+} to Fe^{4+} to maintain charge neutrality, although definitive experiments have not yet been performed. Other possibilities are Pb^{4+}-Pb^{2+}, Pb^{4+}-Fe^{2+} or Pb^{4+}-Yb^{2+} combinations.

The technique used for the microprobe analysis of these films has been described in Reference 14, and the results are shown in Table VI. In the films grown in the BaO-based solution, α_{Ga}[6] is constant and close to unity over a large range of garnet compositions and growth temperatures. The distribution coefficients of the rare earths are also constant and increase with increasing ionic radius, which is consistent with the observations of Van Uitert[1] and Giess.[6] For the films grown in the $PbO-B_2O_3$ solvent, α_{Ga} = 2.03, twice the value in the BaO-based solvent, but the distribution coefficients of the rare earth ions are very similar to those in the BaO-based solvent. No Ba was detected in the analysis but 0.18 wt. % Pb was found, in agreement with the emission spectrographic analysis.

Table VI. Garnet Film Compositions

Solvent (mole %)	Solution Composition/ Solid Composition	Growth Temperature/ Growth Time	Thickness (μm)	Lattice Parameter (Å)	a_{Ga}	a_{Gd}	a_{Y}	a_{Yb}
41% BaO, 41% B_2O_3	$Gd_{1.28}Y_{.98}Yb_{.73}Ga_{.90}Fe_{4.1}O_{12}$	1030°C	9.0	12.393	0.88	1.15	0.96	0.81
18% BaF_2	$Gd_{1.47}Y_{.94}Yb_{.59}Ga_{.80}Fe_{4.2}O_{12}$	30 min.						
"	$Gd_{.98}Y_{1.27}Yb_{.75}Ga_{.90}Fe_{4.1}O_{12}$	1040→990°C	4.0	12.390	0.95	1.22	0.84	0.83
	$Gd_{1.20}Y_{1.17}Yb_{.62}Ga_{.85}Fe_{4.15}O_{12}$	29 min.						
"	$Gd_{.85}Y_{1.40}Yb_{.75}Ga_{.90}Fe_{4.1}O_{12}$	990°C	4.1	12.374	0.97	1.20	0.80	0.80
	$Gd_{1.02}Y_{1.38}Yb_{.60}Ga_{.87}Fe_{4.13}O_{12}$	15 min.						
"	$Gd_{.70}Y_{1.55}Yb_{.75}Ga_{.90}Fe_{4.1}O_{12}$	1040→990°C	3.6	12.370	0.99	1.21	0.83	0.83
	$Gd_{.86}Y_{1.52}Yb_{.62}Ga_{.89}Fe_{4.11}O_{12}$	20 min.						
94% PbO,	$Gd_{.70}Y_{1.55}Yb_{.75}Ga_{.46}Fe_{4.54}O_{12}$	900°C	4.6	12.380	2.03	1.17	1.05	0.73
6% B_2O_3	$Gd_{.82}Y_{1.63}Yb_{.55}Ga_{.93}Fe_{4.07}O_{12}$	15 min.						

3.3. Lattice Parameter

The lattice parameters of the garnet films were determined by a method similar to that developed by Pierron and McNeely for semiconductor single crystals.[15] $Mo_{K\alpha}$ radiation (λ = 0.709261Å) was used to generate the (8,8,8), (12,12,12) and (16,16,16) reflections.

The accuracy of the technique depends upon the separation of the film and substrate peaks. For a lattice mismatch $|\Delta a_0|$ >0.006Å, the peaks can be resolved and the uncertainty in a_0 and Δa_0 is ±0.001Å. For $|\Delta a_0|$ <0.006Å, the peaks merge into one broad peak, and only a qualitative estimate of a_0 and Δa_0 can be made. The uncertainty in this case can be as much as ±0.005Å. For very small mismatch, however, the peaks superimpose into one narrow peak, whose position can once again be determined to ±0.001Å.

The lattice parameter was calculated for each of the peaks and treated analytically to derive a linear expression based on the function $\cot^2 \theta$.[14] This allowed extrapolation to $2\theta = 180°$ where the systematic errors such as absorption, use of a flat specimen, and vertical divergence become negligible. The data were fitted to the expression by a least squares treatment to minimize the effect of random errors. The internal accuracy of the technique, which is dependent on the alignment of both the diffractometer and the crystal in the X-ray beam, was checked by measuring the lattice parameter of a wafer of high quality silicon.

Table VI indicates that garnets of similar composition grown in the PbO-based and BaO-based solvent have quite different measured lattice parameters even though the calculated lattice parameter based on linear interpolation between selected values for the end members was ~12.370Å for both. The uncertainty in the lattice parameter of the 12.380Å film grown in

the PbO-based film is fairly large (±0.005Å) because the peaks could not be resolved, but the difference is still significant and is attributed to the 0.2 wt. % Pb in this film. The increase in lattice parameter with Pb incorporation is in agreement with literature data.[12]

The lattice parameter should change with growth rate and growth temperature if the distribution coefficients of the cations vary with these growth parameters. It has been reported that the distribution coefficient of gallium in particular is very sensitive to both growth rate and temperature in the PbO-B_2O_3 solvent.[6] We have found a reproducible reduction in lattice parameter of 0.003Å for films grown from the same solution of PbO-B_2O_3 at the same temperature (900°C) when the growth rate decreased from 0.95 μm/min to 0.83 μm/min (a decrease of 13%). This corresponds to an increase in Ga content of 0.2 atoms per formula unit[16] and is consistent with an attendant decrease in $4\pi M_s$ and Néel temperature in these films as will be discussed in Section 3.5.

In the BaO-based solvent, the growth rate was varied from 0.2 μm/min to 1.12 μm/min at a growth temperature of 1020°C with no

change in lattice parameter and only a slight change in magnetic properties with growth rate, which indicates that the distribution coefficients are insensitive to growth rate in this solvent. Another set of experiments in which the growth temperature was varied from 990°C to 1050°C (for the same saturation temperature of ∿1060°C) did reveal a change in lattice parameter with an attendent systematic variation in magnetic properties, as will be discussed in Section 3.5.

3.4 Optical Measurements

A double beam spectrophotometer was used to measure the transmittance of garnet epitaxial films of similar composition grown from the BaO-based and PbO-based solvents. For these measurements the absorption coefficient α was calculated from the formula

$$I/I_o = \frac{(1-R)^2 e^{-\alpha t}}{1 - R^2 e^{-2\alpha t}} \qquad (3)$$

where t was taken to be the sum of the film thickness on both sides of the substrate (7-9μm) and R is the reflectance. R was measured to be 0.136 in the wavelength region 2.0-2.5 μm where α for the garnets is negligible, and this value was used in subsequent calculations over the whole spectrum. Since R is a function of wavelength and Equation 3 is strictly valid only for single layer films, this procedure introduces small errors over most of the spectrum with larger error at the absorption edge. The curves for the epitaxial films grown in the different solvents shown in Figure 8 are qualitatively similar. The peaks at 0.9μm and 0.6μm are caused by transitions in the crystal field levels of Fe^{3+} in octahedral and tetrahedral sites, and the shape of the curves is similar to that reported for $Y_3Fe_5O_{12}$.[17] The epitaxial film grown in the PbO-based solvent has an absorption coefficient up to an order of magnitude larger in the visible-near IR region of the spectrum than

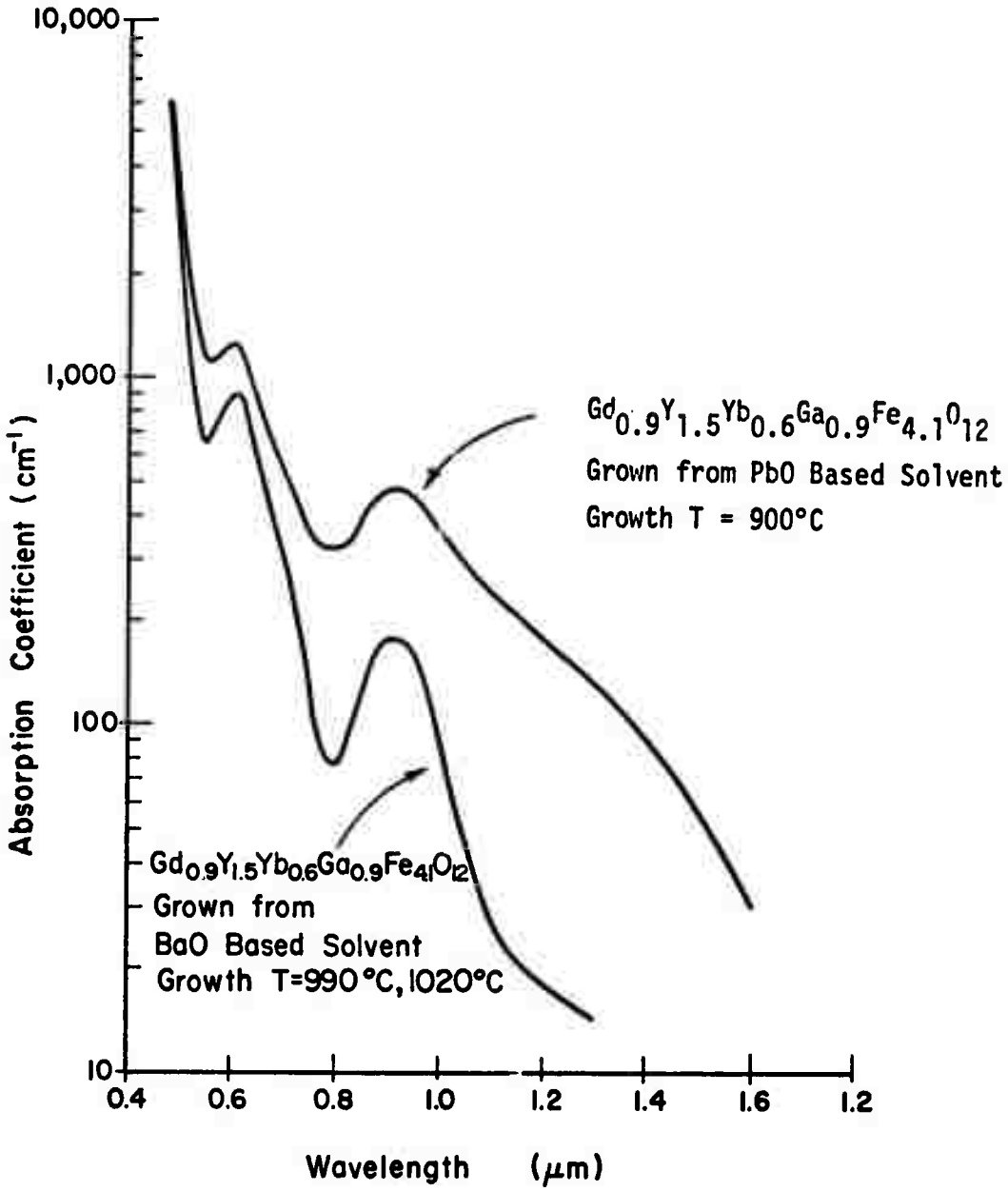

Figure 8. Optical Absorption Curves for Garnet Films.

the film grown from the BaO-based solution. This is attributed to Pb incorporation which probably changes the valence state of Fe, leading to increased absorption.[18] There was no significant change in absorption for films grown in in BaO-based solution at 990°C and 1020°C. The films grown in the $PbO-B_2O_3$ solution were reddish in color as they were withdrawn from the furnace, changing to the characteristic olive green as they cooled to room temperature, corresponding to a shift in the position of the absorption peaks from higher to lower wavelength as the temperature decreased. A similar change in coloration was detected in the films grown in the BaO-based solution, whose color was a much lighter shade of green (for the same film thickness) than those grown from the PbO-based solution. The optical properties of the magnetic films are not critical for magnetic bubble devices, but may be of importance in magneto-optic applications.

3.5 Film Thickness and Magnetic Characterization

The techniques used for the measurement of film thickness as well as the magnetic measurements are listed in Table VII. The details of these techniques, except for the bubble translation technique, have been described in Reference 4.

A variety of properties of representative films grown from BaO-based and PbO-based solvents are shown in Table VIII. The first four runs, B1, B2, B3 and B4 show the effect of varying growth rate in the BaO-based solvent at a 1020°C growth temperature. The growth rate was varied by adjusting the rotation rate of the horizontally held substrates from 0-200 rpm. Although the growth rate varies by a factor of 4, the variation of magnetic properties shows only a slight trend. The Néel temperature and lattice parameter are constant within the accuracy of the measurement indicating that the total gallium distribution

Table VII.

Characterization Techniques for Magnetic Rare Earth Iron Garnets

Parameter	Current HPL Method	Estimated Error in Analysis
1. Substrate and film surface perfection	Etch pit studies, Berg-Barrett and Lang topography, optical microscopic mapping, scanning electron microscopy	-
2. Impurity analysis	Emission spectroscopy, microprobe analysis	±10%
3. Film composition and compositional homogeneity	Microprobe, lattice parameter measurement, calculate from magnetization and Neél temperature	±10%
4. Film-substrate lattice parameter difference and film lattice parameter	X-ray diffractometry	Varies from ± .001Å to ± .005Å depending on mismatch
5. Film thickness and thickness uniformity	Metallographic cross section, interferometry	±10%
6. Magnetization	Static collapse of bubbles, Stripe domain width	±15%
7. Characteristic length	Stripe domain width	±5%
8. Wall energy	Calculate from $\sigma_w = 4\pi M^2 \ell$	±15%
9. Anisotropy constants	Torque magnetometer	±20%
10. Mobility	Bubble translation	±20%
11. Coercive force	AC optical modulation, bubble translation	±15%
12. Neél Temperature	Faraday effect domain observation in hot stage microscope	±1°C
13. Stripe width temperature coefficient	Faraday effect domain observation in hot stage microscope	±10%
14. Index of refraction	Brewster angle	±5%

coefficient α_{Ga} as well as the rare earth distribution coefficients are not sensitive to growth rate. However, the magnetization does increase slightly with increasing growth rate, which results in a decrease in the characteristic length. These results are also evident in Table V and Figure 6, and can be explained as follows. The magnetization is lowered in the material by gallium substitution in tetrahedral sites, and the percentage of gallium in tetrahedral sites is normally ~91%.[12] This distribution can be considered an ordering phenomenon analogous to the growth induced ordering of rare earth ions which causes growth induced anisotropy. At faster growth rates, there is less ordering because there is less time available for atomic arrangement. As a result, the distribution of gallium in octahedral and tetrahedral sites becomes more random, the percentage of gallium in octahedral sites goes up, and as a result the magnetization increases. This effect may occur in the PbO-based solvent as well, but is obscured there by a gross change in the total gallium distribution coefficient.[6]

Runs B2, B5, B6 and B7 show the effect of changing growth temperature (hence supersaturation) on the magnetic properties (at constant rotation rate). Although the growth rate also varied in these experiments, as just shown it has a minor effect on magnetic properties. The variation seen in lattice parameter and magnetic properties, particularly in Néel temperature, where T_N varies from 170°C to 159°C for a change in growth temperature T_G = 990°C to T_G = 1050°C, is attributed to an increase in α_{Ga} with increasing growth temperature. The insensitivity of α_{Ga} to growth rate allows the magnetic properties to be tailored in the BaO-based solution merely by adjusting the growth temperature.

Table VIII. Properties of Epitaxial Layers Grown in $BaO-B_2O_3-BaF_2$ and $PbO-B_2O_3$ Solvents

Run Number	Solvent	Solute Composition	Growth Temp. (°C)	Growth Rate (μm/min)	Thickness (μm)	Lattice Parameter (Å)	ℓ (μm)	$4\pi M$ (Gauss)	σ_w (ergs/cm²)	T_N (°C)
B1	$BaO-B_2O_3-BaF_2$	$(Gd_{.7}Y_{1.55}Yb_{.75})(Ga_{.9}Fe_{4.1})O_{12}$	1020°C	.76	5.8	12.370	.44	187	.12	164
B2	"	"	"	0.70	3.5	12.371	.47	166	.11	163
B3	"	"	"	0.43	3.3	12.370	.54	147	.093	162
B4	"	"	"	0.24	1.8	12.370	.57	159	.11	163
B5	"	"	990	1.02	5.1	12.373	.30	220	.12	170
B6	"	"	1040	0.29	2.9	12.372	.69	139	.11	159
B7	"	"	1050	0.13	3.0	12.371	.90	109	.085	159
B8	"	"	1040-990	0.20	3.6	"	.80	124	.098	163
P1	$PbO-B_2O_3$	" $(Ga_{.46}Fe_{4.54})O_{12}$	900	.95	3.7	12.381	.23	250	.116	157
P2	"	" $(Ga_{.48}Fe_{4.52})O_{12}$	"	"	3.8	12.382	.42	175	.102	152
P3	"	" $(Ga_{.50}Fe_{4.50})O_{12}$	"	"	3.7	12.380	.55	152	.101	148
P4	"	" $(Ga_{.52}Fe_{4.48})O_{12}$	"	"	3.7	12.376	.80	115	.084	146
P5	"	"	"	.83	3.3	12.373	1.10	103	.093	144

Runs P1, P2, P3 and P4 were grown in the $PbO-B_2O_3$ solvent and illustrate the effect of increasing solution gallium content at a 900°C growth temperature without changing any other growth parameters. The lattice parameter decreases (although the superposition of peaks in runs P1, P2, and P3 makes quantitative determination difficult) and the Néel temperature drops with an attendent decrease in $4\pi M$ and an increase in characteristic length. The growth rate of run P5 decreased slightly because of spontaneous nucleation elsewhere in the solution, resulting in a sharp decrease in gallium content in the film as evidenced by the lower Néel temperature. The data shown for runs P4 and P5 indicate that the characteristic length in the PbO-based solvent decreases by $\sim$0.3 μm for an increase in growth rate of 0.1μm/min. In Section 2.2.2 it was shown that the characteristic length decreased by $\sim$0.025 μm for a similar increase in growth rate in the BaO-based solvent, which represents more than an order of magnitude greater insensitivity in the $BaO-B_2O_3-BaF_2$ solvent.

The bubble translation technique was used for the measurement of bubble mobility and coercivity because it simulates conditions in an actual device.[19] In this technique a bubble is moved at constant diameter by applying a pulsed magnetic gradient of known magnitude and duration. The velocity and mobility of the bubble and the coercive force in the film can be calculated from the bubble diameter and the distance that it moves. Films grown in either solvent exhibited a limiting velocity of 20-30 m/sec as shown in Figure 9. The film shown has an initial mobility of 1740 cm/Oe-se and its coercive force is 0.03 Oe. The coercive force is consistently lower in the Bao-based solvent.[20] The reasons for this are not clear but the higher coercive force in films grown in $PbO-B_2O_3$ may be a consequence of the higher impurity content in these films.

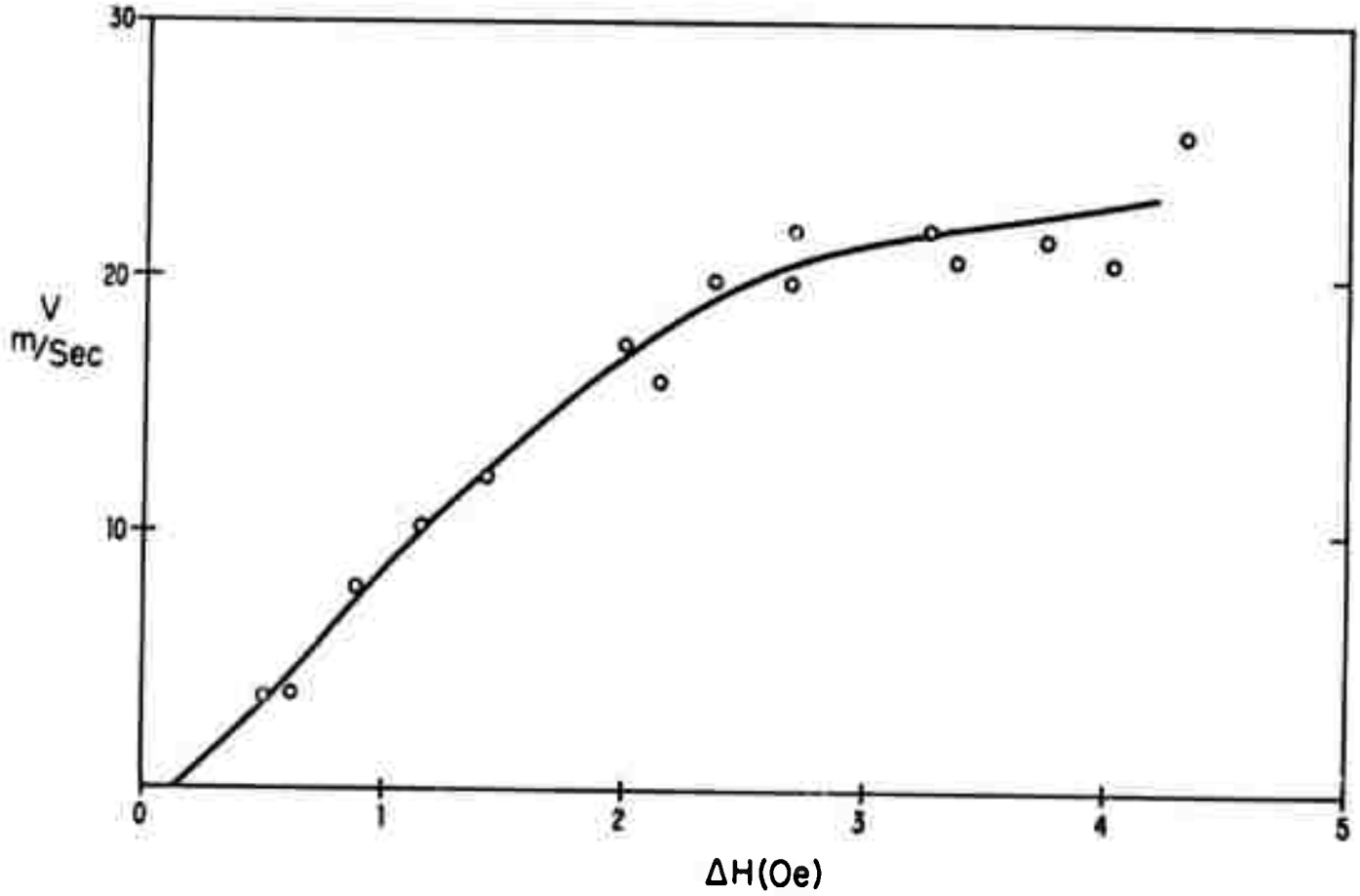

Figure 9. Magnetic Bubble Velocity in $(Gd,Y,Yb)_3$ $(Ga,Fe)_5O_{12}$ Grown in $BaO-B_2O_3-BaF_2$ Solvent as a Function of Drive Field Determined by the Bubble Translation Technique.

Other magnetic properties of films of similar composition grown in the BaO-based and PbO-based solvents are similar even though the growth temperature, solvent impurity content and the resultant lattice parameters and optical properties are quite different as shown in Table IX.

Table IX. Comparison of Properties of Bubble Garnets Grown in BaO-based and PbO-based Solvents

PROPERTY	$BaO-B_2O_3-BaF_2$ SOLVENT	$PbO-B_2O_3$ SOLVENT
Solid Composition	$Gd_{.86}Y_{1.52}Yb_{.62}Ga_{.89}Fe_{4.11}O_{12}$	$Gd_{.82}Y_{1.63}Yb_{.55}Ga_{.93}Fe_{4.07}O_{12}$
Lattice Parameter	12.370Å	12.380 Å
Thickness ± Variation Over Central cm^2	3.6 ±0.15 μm	4.6 ±0.15 μm
Growth Temperature	1040 → 990°C	900°C
Growth Rate	0.16 μm/min.	0.31 μm/min.
Characteristic Length	0.80 μm	0.73 μm
Magnetization	150 Gauss	127 Gauss
Anisotropy Field	695 Oe	640 Oe
Mobility (Initial)	1500 cm/Oe-sec	1500 cm/Oe-sec
Coercive Force	0.04 Oe	0.11 Oe
Néel Temperature	164°C	154°C
Defect Density	< $20/cm^2$	< $20/cm^2$

SECTION IV

4.0. CONCLUSIONS

Reproducible growth of the rare earth iron garnet $(Gd,Y,Yb)_3(Ga,Fe)_5O_{12}$ has been demonstrated in both $BaO-B_2O_3-BaF_2$ and $PbO-B_2O_3$ solvents. The BaO-based solvent has been characterized, suitable garnet growth parameters have been developed, and the effect of varying these growth parameters upon the garnet composition and magnetic properties has been investigated. One of the most significant factors to emerge is the relative insensitivity of the magnetic properties of garnet films grown in the BaO-based solvent to changes in growth rate. One of the contributing factors is the higher viscosity of this solvent compared to the PbO-based solution, although a completely satisfactory explanation has not yet been found.

The defect densities are comparable in films grown in the two solvents, but the defect morphology is considerably different. Although all of the defects are pits, these can be caused either by substrate defects or by tiny crystallites of garnet or orthoferrite embedded in the film, and further work is necessary to quantitatively describe these defects.

Lattice parameter and optical measurements indicate a higher lattice parameter and higher optical absorption coefficient for garnet films of similar composition grown in the PbO-based solvent. These results are consistent with the higher solvent impurity content of the films grown in the PbO-based solvent, and may have implications for magneto-optic applications. Even though these properties are different, the magnetic properties of the films are comparable.

REFERENCES

1. L. G. Van Uitert, W. A. Bonner, W. H. Grodkiewicz, L. Pictroski and G. J. Zydzik, Mat. Res. Bull. 5, 825 (1970).

2. R. A. Burmeister, T. L. Felmlee and R. Hiskes, Final Technical Report, Magnetic Rare Earth Compounds, Contract No. DAAH01-70-C-1106, June 1971.

3. R. Hiskes and R. A. Burmeister, to be published in J. Electronic Materials.

4. R. Hiskes and R. A. Burmeister, Final Technical Report, Magnetic Rare Earth Compounds II, Contract No. DAAH01-C-1259, June, 1972.

5. R. Hiskes and R. A. Burmeister, to be published in American Institute of Physics Proceedings of Eighteenth Annual Conference on Magnetism and Magnetic Materials, 1972.

6. E. A. Giess, J. D. Kuptsis and E. A. D. White, J. Crystal Growth 16, 36 (1972).

7. R. Ghez and E. A. Giess, to be published in Mat. Res. Bull.

8. J. R. Carruthers and K. Nassau, J. Appl. Phys. 39, 5205 (1968).

9. J. A. Burton, R. C. Prim and W . P. Slichter, J. Chem. Phys. 21, 1987 (1953).

10. R. A. Burmeister, T. L. Felmlee and R. Hiskes, Semiannual Technical Report, Magnetic Rare Earth Compounds, Contract No. DAAH01-70-C-1106 December, 1970.

11. J. C. Brice, J. Crystal Growth 1, 218 (1967).

12. L. S. Blank and J. W. Nielsen, presented at 18th Annual Conference on Magnetism and Magnetic Materials, Denver, Colorado, November 1972.

13. M. Kestigian, J. Am. Ceram. Soc. 50, 165 (1967).

14. R. Hiskes and R. A. Burmeister, Semiannual Techical Report, Magnetic Rare Earth Compounds, Contract No. DAAH01-71-C-1259, February 1972.

15. E. D. Pierron and J. B. McNeely,"Advances in X-ray Analysis,"Vol. 12, C. S. Barrett, J. B. Newkirk, and G. R. Mallett, Eds., Plenum Press, New York, 1969, 343-353.

Preceding page blank

16. E. A. Giess, B. E. Argyle, D. C. Cronemeyer, E. Klokholm, T. R. McGuire, D. F. O'Kane, T. S. Plaskett and V. Sandagopan, AIP Conf. Proc. No. 5, Magnetism and Magnetic Materials Conference, Chicago (Nov. 1971), (A.I.P., N.Y., 1972), p. 110.

17. D. L. Wood and J. P. Remeika, J. Appl. Phys. 38, 1038 (1967).

18. L. E. Sobon, K. A. Wickersheim, J. C. Robinson and M. J. Mitchell, J. Appl. Phys. 38, 1021 (1967).

19. G. P. Vella-Coleiro and W. J. Tabor, Appl. Phys. Lett. 21, 7 (1972).

20. R. B. Clover, L. S. Cutler and R. F. Lacey, to be published in American Institute of Physics Proceedings of the Eighteenth Annual Conference on Magnetism and Magnetic Materials 1972.